

An Annual Report for  
**ION DOPED QUANTUM  
WELL LASERS**

DTIC  
ELECTE  
FEB 28 1995  
S G D

Submitted under  
Contract No. F49620-93-C-0001

Submitted to  
**Air Force Office of Scientific Research/PKC**  
**110 Duncan Avenue, Suite B115**  
**Bolling AFB, DC 20332-0001**

**DISTRIBUTION STATEMENT A**

Approved for public release;  
Distribution Unlimited

DTIC



**spire**

**19950209 057**

An Annual Report for:  
ION DOPED QUANTUM WELL LASERS



Report period  
30 September 1993 through 30 September 1994

Submitted under:  
Contract No. F49620-93-C-0069

Submitted to:  
Air Force Office of Scientific Research/PKC  
110 Duncan Avenue, Suite B115  
Bolling AFB, DC 20332-0001

Submitted by:  
Spire Corporation  
One Patriots Park  
Bedford, MA 01730-2396

Accession For	
NTIS CRA&I	<input checked="" type="checkbox"/>
DTIC TAB	<input type="checkbox"/>
Unannounced	<input type="checkbox"/>
Justification	
By	
Distribution /	
Availability Codes	
Dist	Avail and/or Special
A-1	

REPORT DOCUMENTATION PAGE			Form Approved OMB No. 0704-0188	
Public reporting burden for this collection of information is estimated to average 1 hour per response, including the time for reviewing instructions, searching existing data sources gathering and maintaining the data needed, and completing and reviewing the collection of information. Send comments regarding this burden estimate or any other aspect of this collection of information, including suggestions for reducing this burden, to Washington Headquarters Services, Directorate for Information Operations and Reports, 1215 Jefferson Davis Highway, Suite 1204, Arlington, VA 22202-4302, and to the Office of Management and Budget, Paperwork Reduction Project (0704-0188), Washington, DC 20503				
1. AGENCY USE ONLY (Leave blank)	2. REPORT DATE 2/6/95	3. REPORT TYPE AND DATES COVERED 9/30/93 to 9/29/95		
4. TITLE AND SUBTITLE Ion Doped Quantum Well Lasers		5. FUNDING NUMBERS F49620-93-C-0069		
6. AUTHOR(S) Anton C. Greenwald, Ph.D.,				
7. PERFORMING ORGANIZATION NAME(S) AND ADDRESS(ES) Spire Corporation One Patriots Park Bedford, MA 01730-2396		8. PERFORMING ORGANIZATION REPORT NUMBER  10154		
9. SPONSORING/MONITORING AGENCY NAME(S) AND ADDRESS(ES) Air Force Office of Scientific Research/PKC 110 Duncan Avenue, Suite B115 Bolling AFB, DC 20332-0001		10. SPONSORING/MONITORING AGENCY REPORT NUMBER		
11. SUPPLEMENTARY NOTES				
12a. DISTRIBUTION/AVAILABILITY STATEMENT  <div style="border: 1px solid black; padding: 5px; width: fit-content; margin: 10px auto;"> DISTRIBUTION STATEMENT A  Approved for public release;  Distribution Unlimited </div>		12b. DISTRIBUTION CODE		
13. ABSTRACT (Maximum 200 words)  <p>The objective of this research project is to fabricate erbium-doped light emitting diode lasers. Such lasers are expected to be temperature independent, frequency stable sources of 1538 nm light especially well suited for optical communications.</p> <p>During the first year of the project new volatile erbium-silylamide sources were synthesized for metalorganic chemical vapor deposition of doped III-V compound films, required for laser fabrication. Doping levels to 30 atomic percent were tested but the maximum substitutional dopant level was 0.02 percent. Carbon and nitrogen contaminant levels were minimized, while the amount of silicon left in the film was a function of deposition temperature. Narrow photo- and cathode-luminescence spectra were obtained from these films. Diffusion rates for erbium in gallium arsenide was higher than expected. Device studies are planned for the second year of the project.</p>				
14. SUBJECT TERMS diode lasers, erbium doped GaAs, rare earth doped GaAs, GaAs, AlGaAs, rare earth doped semiconductors, metalorganic erbium compounds, volatile erbium compounds			15. NUMBER OF PAGES	
			16. PRICE CODE	
17. SECURITY CLASSIFICATION OF REPORT Unclassified	18. SECURITY CLASSIFICATION OF THIS PAGE Unclassified	19. SECURITY CLASSIFICATION OF ABSTRACT Unclassified	20. LIMITATION OF ABSTRACT Unlimited	

## SUMMARY

Solid-state diode lasers are very small, bright, inexpensive sources of coherent light but are characterized by a temperature-dependent emission wavelength. Typically, variations of 0.3 nm shift in output wavelength per degree Celsius change in temperature are observed. If frequency stability is required, as in matching wavelengths to fiber-optic amplifiers, relatively bulky, power consuming thermoelectric coolers are necessary.

Lasers driven by ion emission are frequency stable. The concept of electrically pumping erbium ions in a semiconductor matrix for frequency stable operation is not new, but laser emission has not been demonstrated. Spire proposed optical pumping of erbium directly in the semiconductor matrix, as opposed to using a semiconductor laser to pump an external cavity laser, for increased efficiency and size reduction.

The objective for the first year of this program was to demonstrate metalorganic chemical vapor deposition (MOCVD) of good quality GaAs films *in-situ* doped with erbium using new source materials. This objective was achieved. Prior work had demonstrated erbium doping of the GaAs lattice but with large amounts of carbon in the matrix. In the Phase I research, Spire showed that this effect was related to the chemistry of the cyclopentadienyl derivatives sources used and that contamination could be substantially reduced with new chemicals. In this work, erbium amides of the form  $\text{Er}\{\text{N}[\text{SiR}_3]_2\}_3$  where R is an organic radical typically  $\text{CH}_3$ ,  $\text{C}_2\text{H}_5$ , were used to dope the semiconductor films.

Spire deposited films with varying erbium concentrations up to thirty atomic percent. Analysis by Rutherford backscattering spectroscopy showed that the maximum amount of erbium substitutional in the film, grown at temperatures up to  $720^\circ\text{C}$ , was  $10^{19} \text{ cm}^{-3}$ , or 0.02 atomic percent. The films were further analyzed by secondary ion mass spectroscopy for low levels of contaminants such as carbon, oxygen, and nitrogen - all found to be negligible - and for silicon. The concentration of Si in the film varied with deposition temperature, being higher for greater deposition temperatures in the range 600 to  $720^\circ\text{C}$ . The best films were characterized by photoluminescent spectroscopy. Narrow emission at  $1.54 \mu\text{m}$  was detected at 77K.

## TABLE OF CONTENTS

	<u>Page</u>
1    PROGRAM GOALS .....	1
2    DESCRIPTION OF RESEARCH .....	3
2.1    Erbium Source Synthesis .....	3
2.1.1    Preparation of $\text{Er}\{\text{N}[\text{Si}(\text{CH}_2\text{CH}_3)_2]_3\}$ .....	3
2.1.2    Preparation of $\text{Er}\{\text{N}[(^t\text{Bu})(\text{Si}(\text{CH}_3)_3)]_3\}$ .....	3
2.1.3    Preparation of $\text{Er}\{\text{N}\{(^t\text{Bu})(\text{SiH}(\text{CH}_3)_2)\}_3\}$ .....	4
2.2    Apparatus .....	5
2.3    Sample Preparation and Analyses .....	7
2.3.1    Methylcyclopentadienyl Erbium .....	7
2.3.2    Tris-trimethyldisilylamido-erbium .....	13
2.3.3    Tris-triethyldisilylamido-erbium .....	22
3    CONCLUSIONS .....	23
4    REFERENCES .....	24

## LIST OF FIGURES

		<u>Page</u>
1	Monolithic AlGaAs diode pumped erbium waveguide laser .....	1
2	Structure of tris- <sup>t</sup> butyltrimethylsilylerbiumamide .....	5
3	Schematic diagram of SPI-MOCVD™ 450 modified for this research .....	6
4	Photoluminescence spectra of sample 1879 at 77K showing a small peak at 1538 nm .....	9
5	Secondary ion mass spectroscopy (SIMS) of samples 1874, 1875, 1876, and 1877, (Table 2) demonstrating variation of erbium doping with process variables .....	10
5	(Cont.) SIMS of samples 1878, 1879, and 1880, demonstrating variation of erbium doping with process variables (Table 2) .....	11
6	SIMS data for sample 1879 showing erbium, carbon, and oxygen profiles .....	12
7	SIMS data for good quantum-well laser wafer fabricated at Spire showing preferred carbon and oxygen levels .....	12
8	Rutherford backscattering spectroscopy (RBS) data for sample 1879 showing erbium peak .....	13
9	SIMS data for sample 1941 with oxygen ion beam .....	15
10	SIMS data for sample 1941 with Cs ion beam .....	15
11	SIMS data for sample 1942 with Cs ion beam .....	16
12	RBS data (top) for sample 1941 and depth-concentration plot interpreted from data (bottom) .....	17
13	Photoluminescence data from samples 2051, 2052, 2053 and 2054 measured at 77K showing clear, sharp peak at about 1538 nm .....	19
14	Cathodoluminescence spectra for sample 2051 at 77K .....	20
15	SIMS data using an oxygen ion beam for samples 2051 and 2052, delivered to AFOSR .....	20

## LIST OF FIGURES (Concluded)

		<u>Page</u>
16	RBS data for sample 2051 showing random and channeling spectra, indicting $\frac{2}{3}$ of the erbium dopant was substitutional .....	21
17	SIMS data of sample 2051, taken with a cesium ion beam showing oxygen and nitrogen levels (left) and silicon and carbon levels (right) .....	21
18	Silicon doping levels as a function of growth temperature for trimethyl-disilylamido-erbium .....	23

## LIST OF TABLES

		<u>Page</u>
1	Time-temperature profiles for GaAs and ErAs deposition with $(\text{MeCp})_3\text{Er}$ .....	7
2	Designed experimental matrix for high concentration Er doping with $(\text{MeCp})_3\text{Er}$ ..	8
3	Time-temperature profiles for GaAs and AlGaAs deposition .....	14



## SECTION 1 PROGRAM GOALS

The overall goal of this program is to fabricate a laser diode whose emission wavelength is stable with respect to changes in temperature. Existing semi-conductor technology uses electronic transitions across the bandgap for optical emission. As the bandgap varies with temperature, a different physical mechanism must be employed for temperature invariant wavelength. Typical solid-state ionic lasers do not show the same temperature variations. Spire proposed to integrate a diode and an ionic laser in one structure (Figure 1) to achieve this goal.

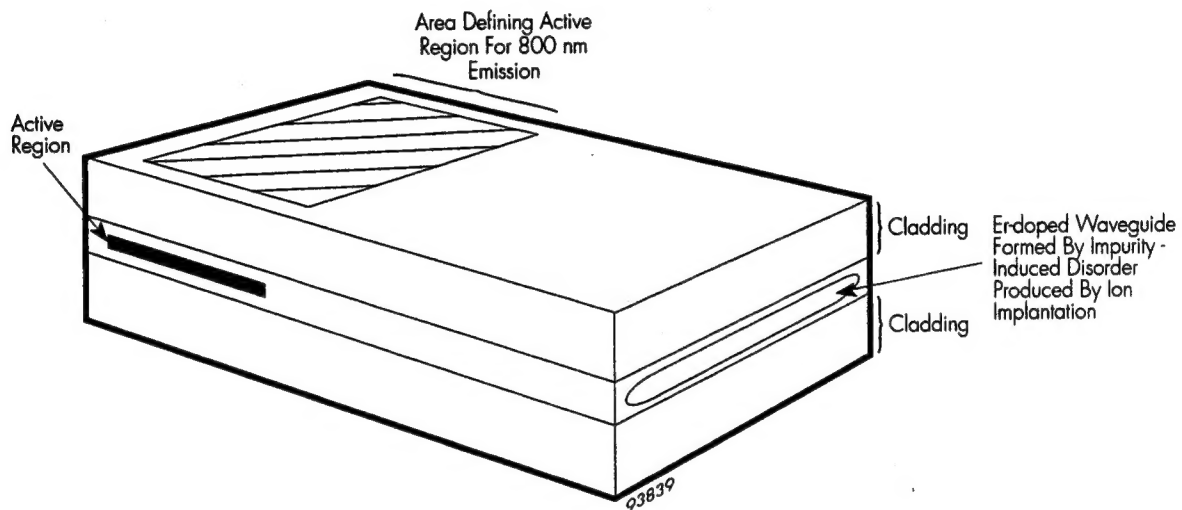


**Figure 1** *Monolithic AlGaAs diode pumped erbium waveguide laser.*

It is considered theoretically possible to pump group IIIA ions in a GaAs matrix electrically, and the cross-section for such an excitation mechanism would be greater than the cross-section for optical pumping.<sup>1</sup> However, an electrically excited ionic laser has not been demonstrated. Only one paper reported electroluminescence of erbium doped GaAs using a reversed biased diode geometry which was inefficient and involved high voltages.<sup>2</sup> Many researchers have reported photoluminescence of erbium doped GaAs and Al GaAs grown by MBE<sup>3,4,5</sup> or by MOCVD.<sup>6,7,8</sup> The reduced risk approach taken by Spire assumes that high intensity light in the waveguide region of a diode laser is sufficient to pump the erbium for lasing at 1.54  $\mu\text{m}$ . The design in Figure 1 allows for a reduced substitutional erbium concentration to be compensated by a longer lasing region. The actively pumped length is kept small to increase efficiency and reduce the heat load that must be removed from the device.



For proper lasing action, the erbium in the GaAs-AlGaAs matrix must be substitutional. An erbium ion emits 1.54  $\mu\text{m}$  only when ionized to the +3 state. Interstitial erbium atoms do not have the right electron coordination. The reported solid solubility of erbium in MOCVD grown GaAs at room temperature is about  $10^{19}/\text{cm}^3$ , which is lower than typical concentrations in glass lasers (about  $10^{20}/\text{cm}^3$ ). To increase gain the length of the optically pumped 1.54  $\mu\text{m}$  emission region is extended in the design of Figure 1.

The technical goal for the first year of this research program was to show that erbium could be incorporated substitutionally in a GaAs and AlGaAs matrix at high concentration without contaminants. Other researchers have grown such material, but with excess carbon doping.<sup>9</sup> Spire was to use new, unique chemical sources for erbium to reduce the contaminant concentration. The specific statement of work was:

- Modify a production aluminum gallium arsenide (AlGaAs) MOCVD reactor to accept volatile erbium (Er) dopants.
- Acquire and evaluate existing volatile erbium compounds for MOCVD growth.
- Dope GaAs and AlGaAs with Er using volatile Er compounds.
  - a) Grow single crystal layers of GaAs and AlGaAs with stoichiometrically incorporated erbium in layers approximately one micron thick.
  - b) Vary the erbium doping levels from zero to approximately 1% atomic concentration.
  - c) Characterize the doped films.
  - d) Deliver two test samples with different Er concentrations to the government for independent verification of erbium incorporation.
- Synthesize and evaluate limited alternate erbium source compounds for MOCVD growth.

Successful erbium incorporation means that single crystal layers of GaAs and AlGaAs have been grown via MOCVD with stoichiometrically incorporated erbium in a concentration and manner which can be verified through analytical means such as secondary ion mass spectroscopy (SIMS), Auger spectroscopy, Rutherford backscattering spectroscopy (RBS), and luminescence.

Spire successfully completed these tasks in the first year of this program.

## SECTION 2 DESCRIPTION OF RESEARCH

### 2.1 Erbium Source Synthesis

Five erbium sources were synthesized for this program, one by Professor R. Kirss of Northeastern University, Boston, one by Gallia, Inc. and the other three by Professor W. Rees, Jr. of Georgia Institute of Technology, the subcontractor to this program. Synthesis of the first source discovered in Phase I was covered in the final report and presented in a paper at the 1993 Materials Research Society Meeting.<sup>10</sup> Synthesis of (MeCp)Er followed routine published reports by Dr. Kriss. Synthesis of other compounds is described below.

All of these compounds are air and moisture sensitive and all manipulations were performed in an inert atmosphere of dry nitrogen or argon using standard Schlenk or glove box techniques. The solvents were degassed and freshly distilled from sodium or potassium benzophenone prior to use.

#### 2.1.1 Preparation of $\text{Er}\{\text{N}[\text{Si}(\text{CH}_2\text{CH}_3)_2]\}_3$

The lithium substituted amide,  $\text{LiN}[\text{Si}(\text{CH}_2\text{CH}_3)_2]_2$  was prepared first. The reaction proceeded in a 500 ml three-necked, round-bottomed glass flask equipped with a reflux condenser, a pressure-equalizing delivery funnel, an internal magnetic stirring bar, a mercury bubbler, and a nitrogen gas inlet. Freshly titrated <sup>n</sup>BuLi/hexanes solution (2.5 moles/l, from Aldrich) was added drop-wise to an initial solution of 24.84 g of hexaethyldisilazine ( $\text{HN}[\text{SiCH}_2\text{CH}_3]_2$ , 101.15 mmole) in 100 ml of diethylether cooled to 0°C. The reaction mixture became increasingly cloudy yielding a white precipitate of the lithium salt at completion. The mixture was slowly warmed to room temperature (1 hour), refluxed for two hours, then stirred for an additional two hours at ambient temperature.

The suspension described above was placed in a 500 ml Schlenk flask, equipped with an internal magnetic stirring bar and a silicon oil bubbler, and cooled to 0°C. Erbium trichloride (9.22g,  $\text{ErCl}_3$ , anhydrous, 33.7 mmole, Strem Chemicals) was added through a canula as a diethylether suspension over a period of two hours. The erbium trichloride and the lithium salt dissolved slowly and the solution became intense pink, accompanied by a precipitation of white lithium chloride. After warming on its own to ambient temperature, followed by stirring for 24 hours, the pink solution was filtered and all volatiles were removed at a reduced pressure of about 20 to 50 torr. The residue was then treated with 200 ml of hexane and filtered from again precipitated lithium chloride. The solvent was distilled off the clear solution and yielded a pink and viscous liquid.

#### 2.1.2 Preparation of $\text{Er}\{\text{N}[(^t\text{Bu})(\text{Si}(\text{CH}_3)_3)]\}_3$

A solution of 45.2g of <sup>t</sup>butylamine ( $^t\text{BuNH}_2$ , 618 mmole) in 650 ml of diethylether cooled to 0°C was prepared in a 1000 ml Schlenk flask equipped with an internal magnetic stirring bar and a silicon oil bubbler. Trimethylchlorosilane (33.5g,  $\text{ClSi}(\text{CH}_3)_3$ , 309 mmole, 39.2 ml) was added very slowly through a syringe. After warming to ambient temperature, the white solid

(<sup>t</sup>butylamine hydrochloride) was removed by Schlenk filtration. The remaining clear solution was distilled at ambient pressure to yield the desired product at 118°C. The yield was 20.6g, or 45.8% of <sup>t</sup>butyltrimethylsilylamine or  $\text{HN}[\{\text{Si}(\text{CH}_3)_3\}(\text{tBu})]$ .

The 20.6g of <sup>t</sup>butyltrimethylsilylamine prepared above was dissolved in 100 ml of diethylether, placed in a smaller 250 ml Schlenk flask equipped with an internal magnetic stirrer and a silicon oil bath, and cooled to 0°C. Then 56.7 ml of a freshly titrated <sup>n</sup>BuLi/hexanes solution (2.5 mole/l) was added over a period of 50 minutes. After warming on its own to ambient temperature, the pale yellow, cloudy solution was refluxed for one hour, then cooled on its own to ambient temperature. The white lithium amide,  $\text{LiN}[\{\text{Si}(\text{CH}_3)_3\}(\text{tBu})]$ , was then purified by recrystallization from an ether/hexane solution. Total yield was 19.47g, or 91%.

The final product was prepared in a 1000 ml, three-necked, round-bottomed flask equipped with a pressure-equalizing funnel, an internal magnetic stirring bar, a silicon oil bubbler, and a nitrogen gas inlet. This flask was initially filled with 11.74g of anhydrous erbium trichloride ( $\text{ErCl}_3$ , 42.9 mmole) dissolved in 300 ml of diethylether and cooled to 0°C. All 19.47g of the lithium amide preparation was dissolved in 100 ml of diethylether and added drop-wise with rapid stirring over a period of two hours. The reaction solution was then warmed to ambient temperature over a period of one hour and stirred for another 12 hours at this temperature. The pink solution was filtered from lithium chloride and all volatiles were removed at reduced pressure. The pink solid residue was subsequently extracted with hexane and filtered from again precipitated lithium chloride. The remaining pink solid was then dried in vacuum ( $10^{-2}$  torr) at about 80°C over a period of 24 hours. Ensuing sublimation at  $10^{-4}$  torr and 100°C gave the desired product, an intense pink colored amorphous powder with a yield of 12.85g (49.9%). NMR spectroscopy results: [ $\text{C}_6\text{D}_6$ ,  $\delta$ , ppm], 0.875 (s, 27H,  $\text{C}(\text{CH}_3)_3$ ); -0.016 (s, 27H,  $\text{Si}(\text{CH}_3)_3$ ).

The structure of tris-<sup>t</sup>butyltrimethylsilylerbiumamide is shown in Figure 2. Preliminary measurements of its vapor pressure at 80, 100, and 130°C are,  $10^{-5}$ ,  $10^{-4}$ , and  $10^{-3}$  torr.

### 2.1.3 Preparation of $\text{Er}\{\text{N}\{\text{tBu}\}(\text{SiH}(\text{CH}_3)_2)\}_3$

In a 1000 ml Schlenk flask, equipped with an internal magnetic stirring bar and a silicon oil bubbler, a solution of 47.83g of <sup>t</sup>butylamine ( $\text{tBuNH}_2$ , 654 mmole) in 700 ml of diethylether was cooled to 0°C and 30.9g of dimethylchlorosilane [ $\text{ClSiH}(\text{CH}_3)_2$ , 327 mmole] was added very slowly through a syringe. After warming to ambient temperature, the white solid (<sup>t</sup>butylamine hydrochloride) was removed by Schlenk filtration. The remaining clear solution was distilled at ambient pressure to yield the desired product,  $\text{HN}\{\text{SiH}(\text{CH}_3)_2\}(\text{tBu})$ , at 103°C with a yield of 13.23g, 30.8%.

The 13.23g of <sup>t</sup>butyldimethylsilylamine was dissolved in 100 ml of diethylether in a 250 ml Schlenk flask with an internal magnetic stirring bar and a silicon oil bubbler cooled to 0°C. Then 40.3 ml of a freshly titrated <sup>n</sup>BuLi/hexanes solution (2.5 mole/l) was added over a period of 30 minutes. After warming on its own to ambient temperature, the pale yellow cloudy solution was refluxed for one hour, then cooled on its own to ambient temperature and stirred for an additional hour. The white lithium amide was then purified by recrystallization from an ether/hexane solution. The yield of  $\text{LiN}\{\text{SiH}(\text{CH}_3)_2\}(\text{tBu})$  was 12.52g, 90%.

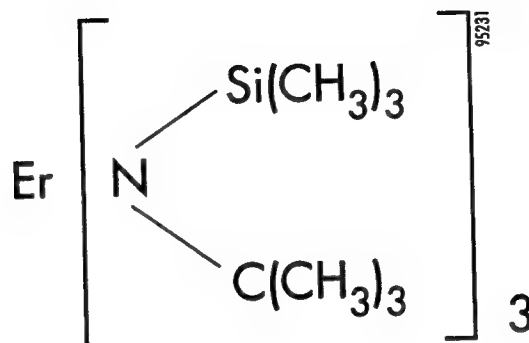
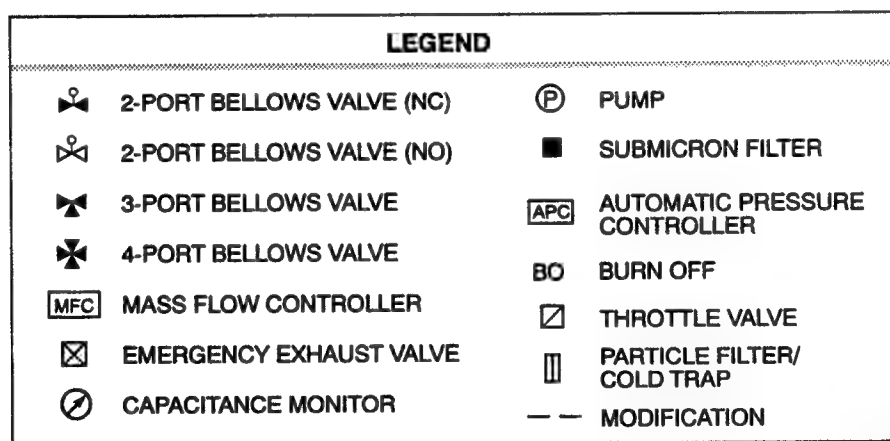
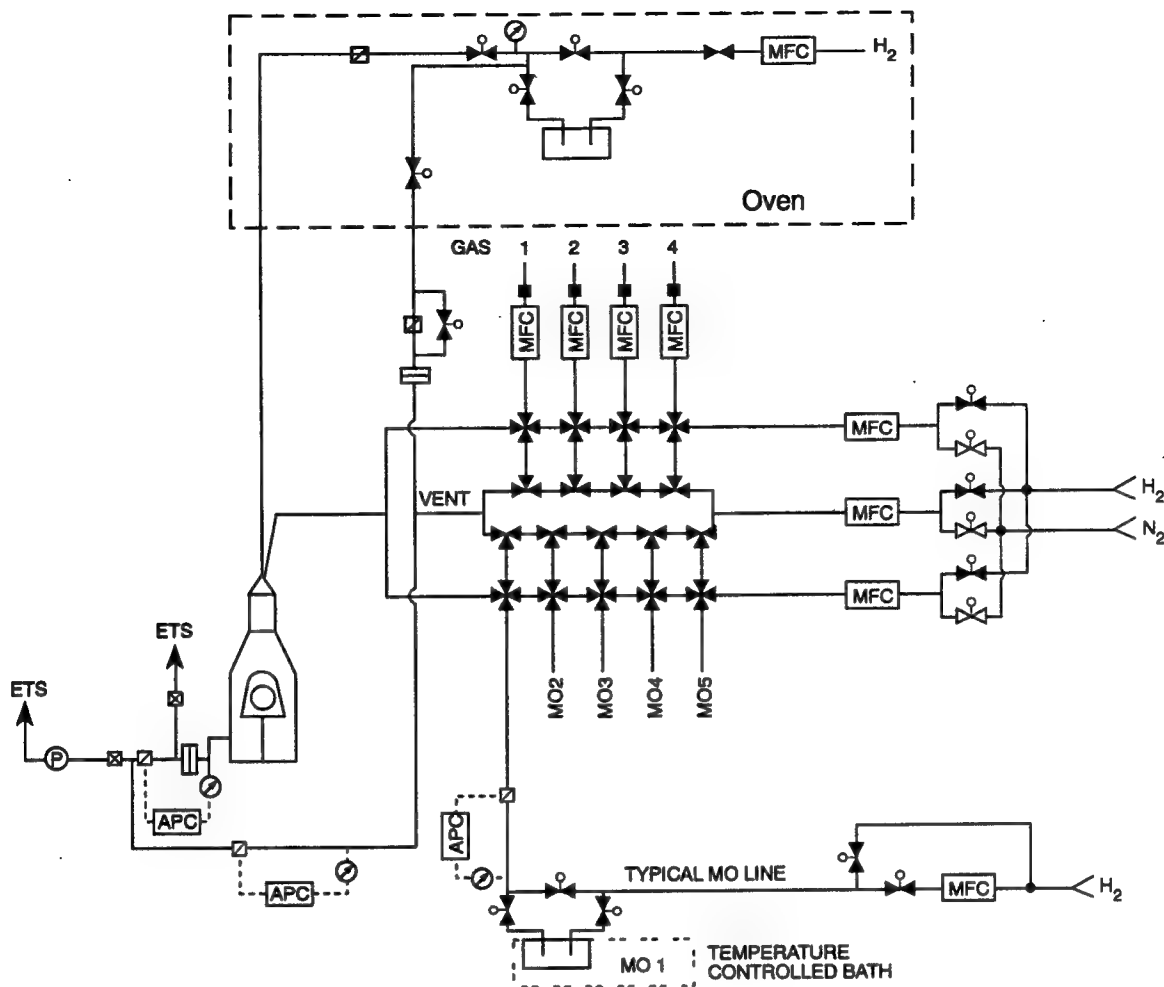


**Figure 2**     *Structure of tris-<sup>t</sup>butyltrimethylsilylerybiumamide.*

The final product was prepared in a 1000 ml, three-necked, round-bottomed flask equipped with a pressure-equalizing funnel, an internal magnetic stirring bar, a silicon oil bubbler, and a nitrogen gas inlet. This flask was initially filled with 8.32g of anhydrous erbium trichloride ( $\text{ErCl}_3$ , 30.4 mmole) suspended in 300 ml of diethylether and cooled to  $0^\circ\text{C}$ . All 12.52g of the lithium amide preparation ( $\text{LiN}\{[\text{SiH}(\text{CH}_3)_2]^t\text{Bu}\}$ , 91.23 mmole) was dissolved in 100 ml of diethylether and added drop-wise with rapid stirring over a period of two hours. The pink reaction solution was then warmed to ambient temperature over a period of one hour and stirred for another 12 hours at this temperature. The reaction mixture was then filtered from lithium chloride and all volatiles were removed at reduced pressure. The residue was subsequently dissolved in 300 ml of hexane and filtered from precipitated lithium chloride. The solvent was reduced to about 100 ml and the remaining pink crystals were washed five times with  $-78^\circ\text{C}$  cold hexane and subsequently dried in vacuum at  $10^{-2}$  torr and  $50^\circ\text{C}$  for 24 hours. The yield was 7.18g at 42%.

## 2.2     Apparatus

The apparatus used for deposition of single crystal GaAs and AlGaAs layers epitaxially on matching substrates by MOCVD is shown schematically in Figure 3. The equipment is installed in a class 1000 clean room, with class 100 curtains for the loading/loading station.



94230

**Figure 3** Schematic diagram of SPI-MOCVD™ 450 modified for this research. All parts in oven were added for this work.

The first task for this program was to modify this reactor to hold high temperature erbium

sources. The added gas network was placed in an oven, shown in Figure 3, for uniform heating of all valves. All valves have metal seals and are rated to over 350°C. Manually operated throttling valves were used to control the pressure because no suitable automated valves for such high temperature service were available. The pressure gauge was mounted outside of the oven with an extension to the carrier line, also because there are no suitable high temperature versions available. For steady operating conditions, the pressure remained stable and did not require frequent adjustment by the operator. All modification work was complete by January 1994.

## 2.3 Sample Preparation and Analyses

Four sets of MOCVD matrix experiments were conducted to deposit erbium doped GaAs and AlGaAs films. The first experimental matrix used methylcyclopentadienyl erbium as a dopant source, the next two data sets used the tris-trimethyldisilylamido erbium source developed in Phase I of this program, while the fourth set tested a tris-triethyldisilylamido-erbium source.

### 2.3.1 Methylcyclopentadienyl Erbium

The designed experimental matrix for testing this source is shown in Tables 1 and 2. Preliminary results with this source indicated that the concentration of erbium in a GaAs film was too low to be detected by SIMS for normal growth rates. To assure that we would see erbium, the gallium source was turned off for part of the run to produce a thin layer of erbium-arsenide. The concentration spike at this point in the growth was seen by RBS as well as SIMS.

**Table 1** *Time-temperature profiles for GaAs and ErAs deposition with (MeCp)<sub>3</sub>Er.*

GaAs		Description of Deposition Steps
Temp. (°C)	Time (sec)	
100	10	purge and start arsine flow
650	600	heat up substrate, Er bypass flowing to reactor
650	15	increase arsine flow
650	120	deposit GaAs or AlGaAs buffer layer
*	900	deposit with Er and arsine only
650	30	deposit capping GaAs or AlGaAs layer
100	900	cool down
100	10	turn off arsine flow and purge

\* See Table 2

**Table 2** *Designed experimental matrix for high concentration Er doping with (MeCp)<sub>3</sub>Er.*

MOCVD Run #	Temp. (°C)	Press. (torr)	Total flow (slpm)	Er carrier (sccm)	AsH <sub>3</sub> flow (sccm)	Film thick. (μm)
1874*	650	50	4	300	175	1.2-1.5
1875*	650	50	4	300	50	.5
1876*	650	50	2	1600	50	.33
1877	650	50	2	800	50	.39
1878	650	200	5	50	50	.24-.36
1879	500	200	5	800	50	.35-.46
1880	500	50	2	50	50	.33-.46
1881	650	200	2	50	335	.33-.55
1882	650	50	5	800	335	.43-.55
1883	500	200	2	800	335	.39
1884	500	50	5	50	335	.39-.52

\* deposition time for erbium layer initially 5, 5, 30, then 15 minutes always

In this experimental matrix, all substrates were half of a two-inch diameter semi-insulating GaAs wafer. The total layer thickness includes the buffer layer which may have more to do with the final measurement than the erbium layer.

Samples were characterized by photoluminescence at Spire Corporation using an argon ion laser at 488 nm and an InSb detector. In addition, most samples were also characterized by SIMS to determine doping levels as a function of depth and low levels of contaminants such as carbon, oxygen, nitrogen, and silicon. RBS was used to calibrate the SIMS data for erbium content, and in the channeling mode to determine relative percentage of substitutional and interstitial erbium.

Photoluminescence data from sample 1879 (see Table 2) are presented in Figure 4. The emission peak at about 1538 nm was barely visible above the background noise level. This reduced luminescence signal was attributed to excess erbium levels near the surface with poor crystal structure.



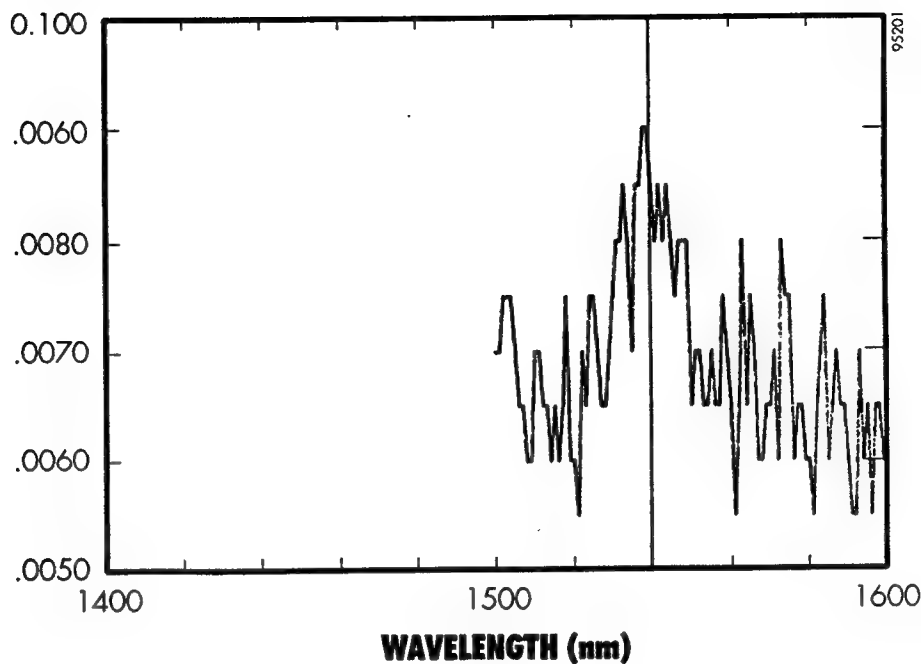


**Figure 4** *Photoluminescence spectra of sample 1879 at 77K showing a small peak at 1538 nm.*

SIMS data using an oxygen ion beam source from samples of run numbers 1875 through 1880 are shown in Figure 5. Data supplied by Analytical Answers Inc., Woburn MA. At high dilution (total gas flow) in the reactor, and intermediate flow through the erbium source, the concentration of erbium in the film was very low (1874, 1875). When the carrier gas flow through the erbium source was significantly increased (1876) the concentration of erbium was significantly increased. Comparing data from samples 1876, 1877, and 1879, the peak concentration for erbium in the film was roughly proportional to the carrier flow through the source. For other samples at low carrier flows, the concentration was again too low to be detected with this technique. These data implied that the amount of erbium doping in the film can be controlled by varying the flow of carrier gas through the source. Very high carrier flow rates were required for a solid source which sublimates at very low vapor pressure.

The analysis compared only the peak heights for the erbium near the surface of the sample. The erbium peak below the surface was an artifact, as discussed previously, created by a dead spot in the erbium feed line which was flushed in a "pulse" during purging of the reactor at the start of the deposition cycle. To some extent, the height of this second, deeper peak was proportional to the settings of the erbium carrier flow.

A second measurement of erbium in sample 1879 was taken by SIMS by Charles Evans and Associates, Inc (Figure 6). This experiment used a cesium ion beam to detect carbon, nitrogen and oxygen levels in the film, but it reduced erbium signal strength (the molecular ion  $\text{ErAs}^+$  was detected). Data agreed with results in Figure 5 for erbium profiles, but also showed relatively large concentrations of carbon and oxygen in the film. For comparison, carbon and oxygen profiles for a good solid-state laser wafer are shown in Figure 7. This erbium source increased contamination levels to unacceptable limits when the erbium concentration was sufficient for laser operation.

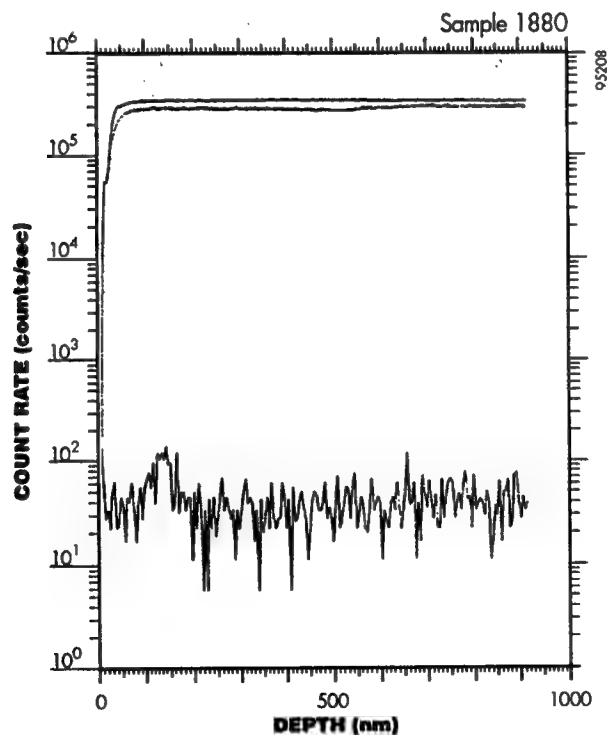
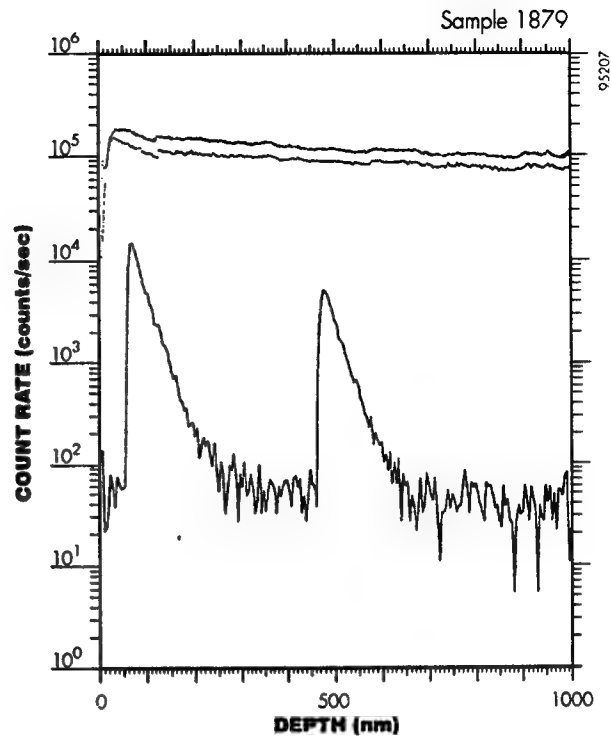
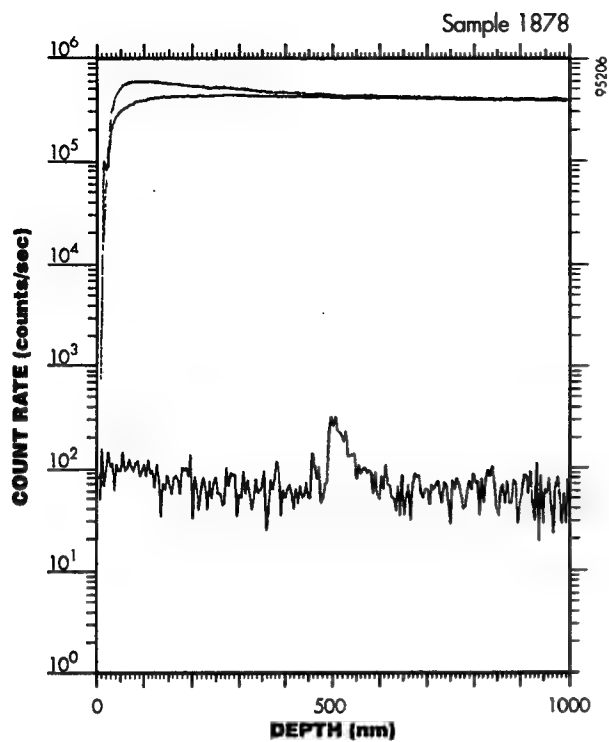


**Figure 5**

(Cont.) SIMS of samples 1878, 1879, and 1880, demonstrating variation of erbium doping with process variables (Table 2).

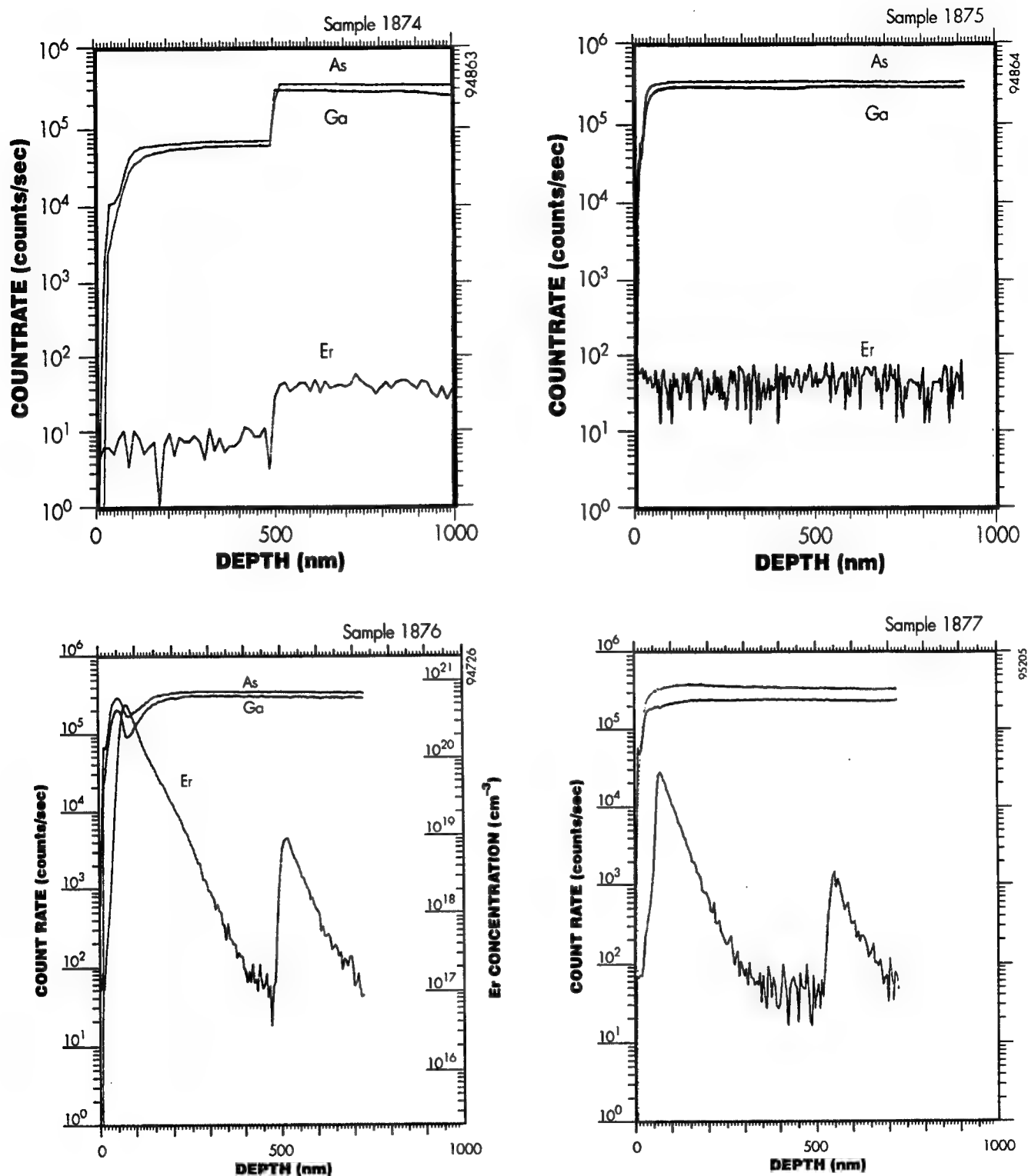


**Figure 5** SIMS of samples 1874, 1875, 1876, and 1877, (Table 2) demonstrating variation of erbium doping with process variables. (Change in sputtering rate on sample 1874 changed signal levels.)

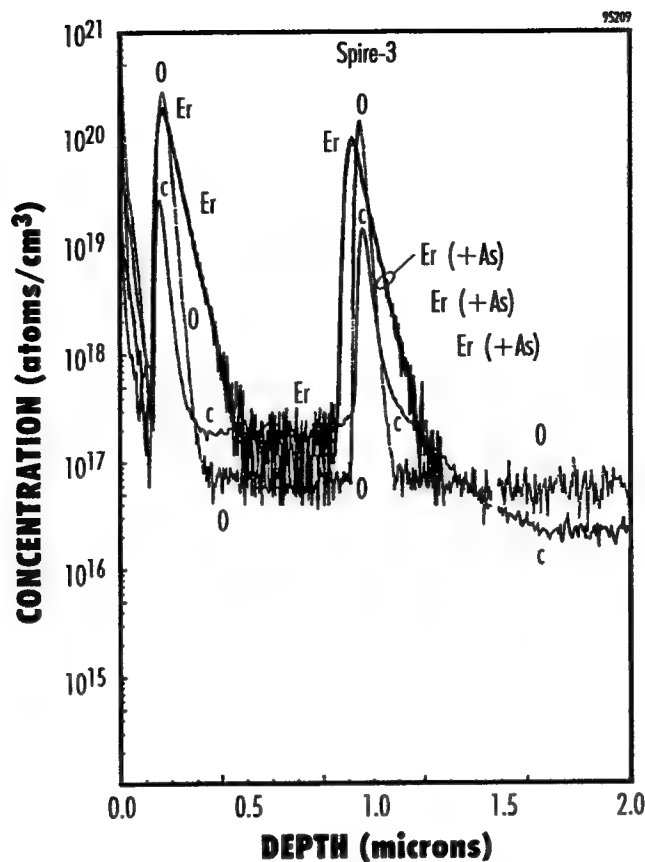


**Figure 6** SIMS data for sample 1879 showing erbium, carbon, and oxygen profiles. Increase in width of erbium peak relative to C and O implies rapid dopant diffusion.

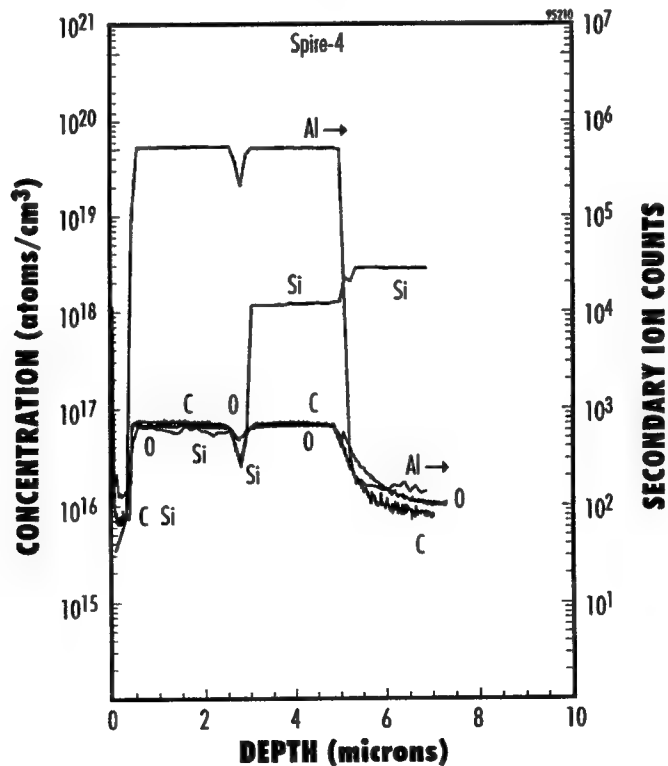


**Figure 7** SIMS data for good quantum-well laser wafer fabricated at Spire showing preferred carbon and oxygen levels.

Calibration of the erbium levels in the SIMS data was determined from the RBS analysis shown in Figure 8 for sample 1879. Only one erbium peak was visible. Either the peak height of the buried layer was too small to be seen at the point where this data was taken (note linear RBS scale as opposed to a logarithmic scale for SIMS), or signals from the two peaks were indistinguishable. The signal level from erbium was about a factor of 200 lower than the signal from Ga or As.

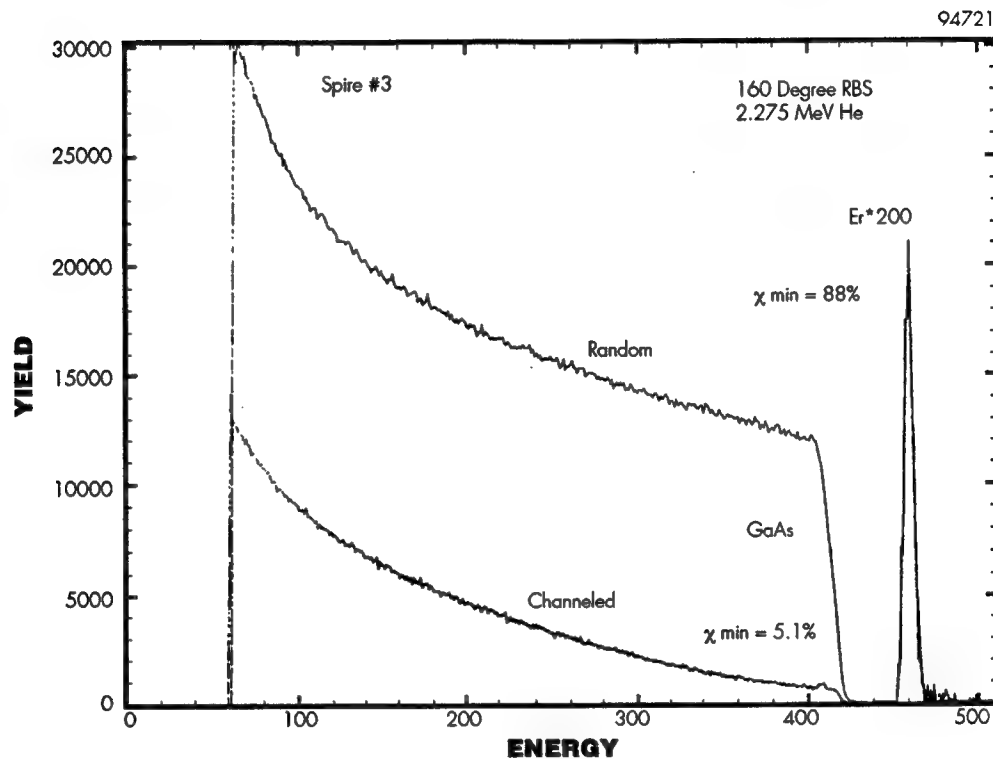


**Figure 8** RBS data for sample 1879 showing erbium peak. This data was used to calibrate the erbium signal in SIMS data.

### 2.3.2 Tris-trimethyldisilylamido-erbium

This was the erbium source developed in Phase I, with a structure is similar to the amide in Figure 1 except that two trimethyl-silyl groups,  $\text{Si}(\text{CH}_3)_3$ , are attached to each nitrogen atom. The material was synthesized by Gallia Corporation, under license to the Univ. of Florida. This invention, patent application in process, arose from funding for this SBIR project.

Spire purchased additional quantities of this source, and in two growth runs doped GaAs and AlGaAs according to the schedule shown in Table 3. The objective of these experiments, with step-wise varying flow rates for the erbium source, was to determine how this parameter affected the level of erbium incorporated into the semi-conductor. The substrates were 2 inch diameter  $\text{N}^+$  ( $1.7$  to  $2.8 \times 10^{18} \text{ Si/cm}^3$ ) GaAs wafers. The surface of the completed structure was not perfectly smooth.

**Table 3** *Time-temperature profiles for GaAs and AlGaAs deposition.*

Step #	GaAs (1941)		AlGaAs (1942)		Description of Deposition Step
	Temp. (°C)	Time (sec)	Temp (°C)	Time (sec)	
1	100	10	100	10	purge and start arsine flow
2	650	600	720	600	heat up substrate, Er bypass flowing to reactor
3	650	15	720	15	increase arsine flow
4	650	120	720	120	deposit GaAs or AlGaAs buffer layer
5	650	120	720	120	deposit GaAs/AlGaAs with 100 sccm Er flow
6	650	120	720	120	deposit GaAs/AlGaAs with 200 sccm Er flow
7	650	120	720	120	deposit GaAs/AlGaAs with 400 sccm Er flow
8	650	600	720	600	deposit with Er (400 sccm) and arsine only
9	650	60	720	60	deposit capping GaAs or AlGaAs layer
10	100	900	100	900	cool down
11	100	10	100	10	turn off arsine flow and purge

These two samples were analyzed by SIMS and RBS as for sample 1879 etc. described above. Figure 9 shows the oxygen ion beam SIMS data for sample 1941 (GaAs), Figures 10 and 11 show the Cs<sup>+</sup> beam SIMS data for both samples, and Figure 12 gives the RBS data, and deduced concentration-depth plot for sample 1941.

At the time these layers were deposited, there was no *a-priori* knowledge of the erbium concentration to expect in the film. Therefore, to assure that the instrumentation would detect some erbium, the last layer was deposited with the flow of gallium turned off. This created the very high erbium concentration (30 atomic %) layer which created the haze on the surface, and prevented RBS from acquiring ion-channeling data to determine the percent of erbium that was substitutional. The layers below the surface are more typical of the target composition. Figures 9 and 12, especially, show a stepped distribution of erbium in the deposited film below the major peak. These steps corresponded to the changes in carrier gas flow shown in Table 3. Thus, Spire demonstrated control of erbium concentration in the film. (The deep lying erbium peak deposited before the buffer layer was caused, as mentioned previously, by rapid purging of a dead spot in the carrier gas flow lines. The problem was fixed after October 1994.)

The level of contaminants in the films in the region of 1 to 6 atomic percent erbium concentration was greater for the AlGaAs structure than for the GaAs structure. Figure 9 showed that the level of carbon stayed at background minimum detectivity (uncalibrated) for this region in GaAs, while Figure 10 showed that the carbon levels are about a factor of ten above the minimum detectable level ( $5 \times 10^{18}/\text{cc}$ ). In the AlGaAs structure the carbon levels were 4 to  $5 \times 10^{20}/\text{cc}$ . The oxygen concentration in Figure 9 had peaks at the surface and at the point of

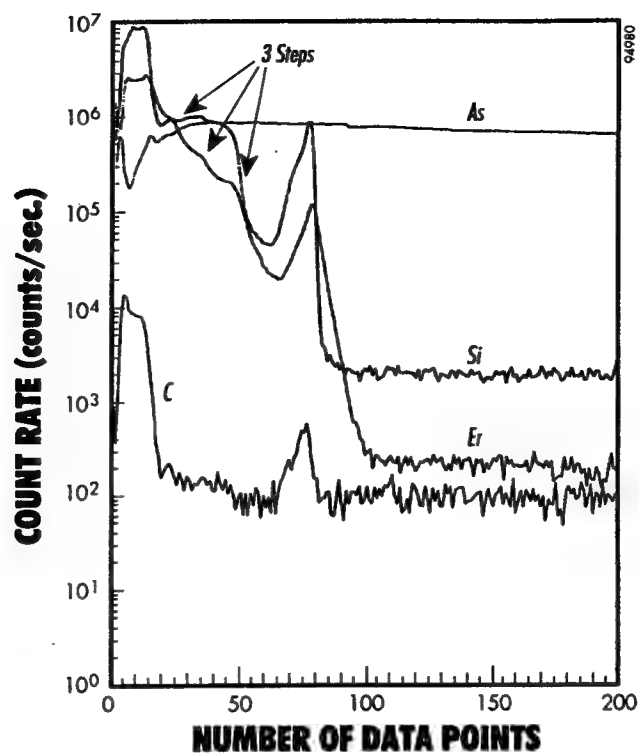


**Figure 9** *SIMS data for sample 1941 with oxygen ion beam. Note that the three steps for the erbium concentration profile lie below the curve for the silicon concentration profile. The ratio of these two elements is NOT calibrated in this data.*

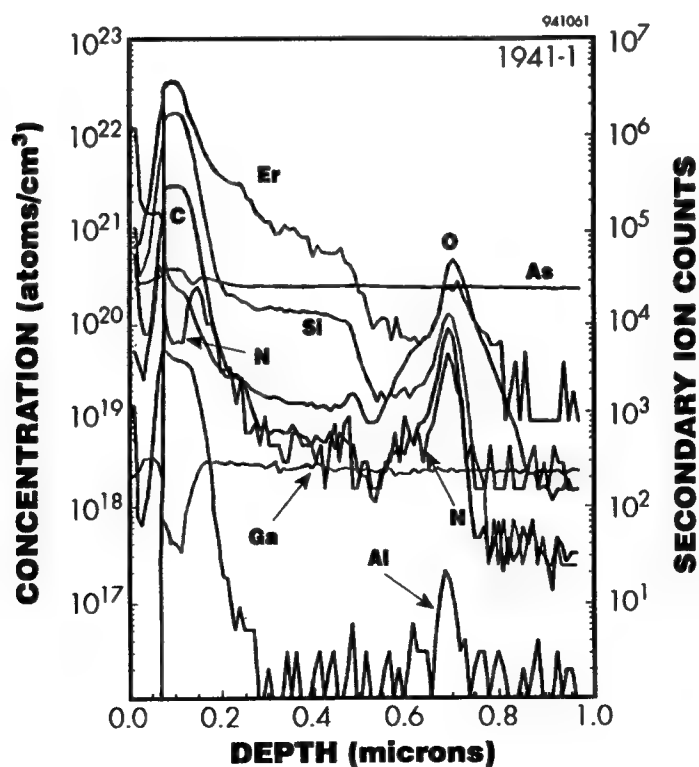


**Figure 10** *SIMS data for sample 1941 with Cs ion beam.*



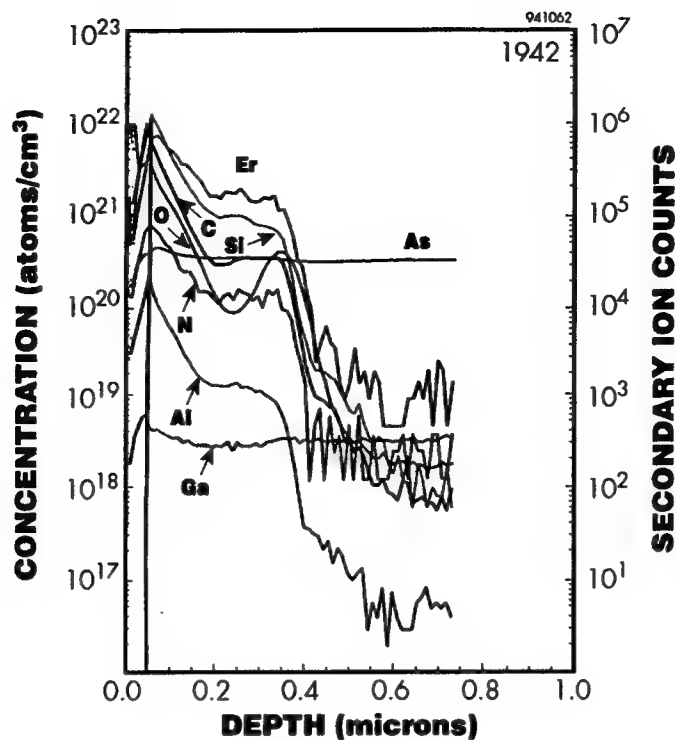


Figure 11 SIMS data for sample 1942 with Cs ion beam.

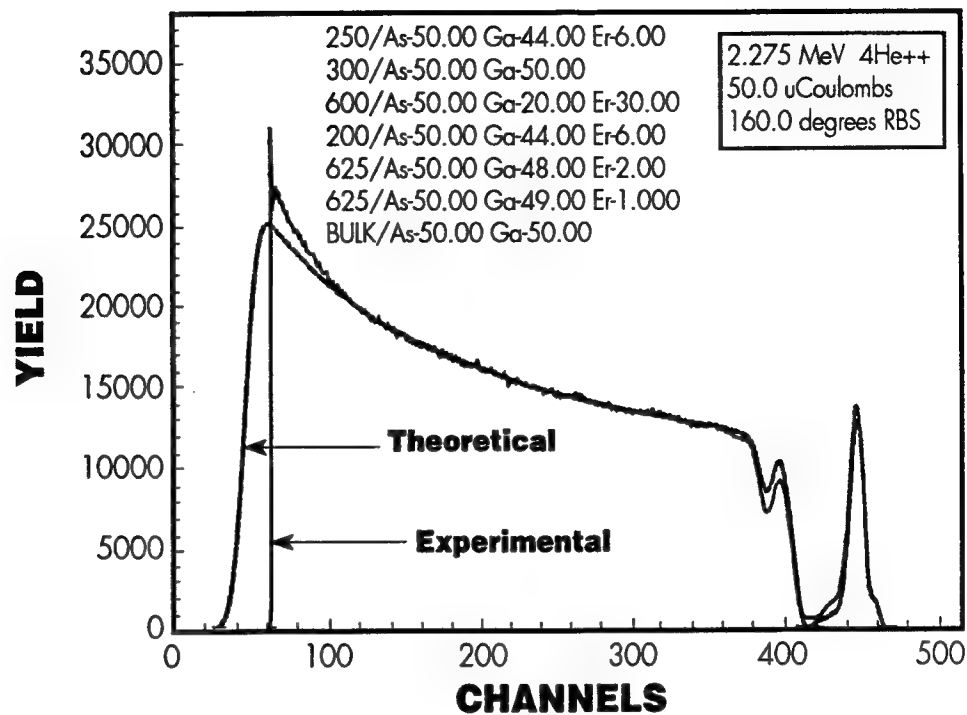
initial growth. Through the lower doped erbium layer the oxygen concentration was less than a factor of ten above the minimal detectable level at about  $10^{19}/\text{cc}$ . the concentration of nitrogen in the GaAs sample was near the minimal detectable levels (sharp spikes are a single ion detected) and could be zero, while in the AlGaAs sample the concentration of nitrogen was over  $10^{20}/\text{cc}$ . Detected levels of silicon followed the same pattern. In GaAs layers the silicon concentration was about  $10^{20}/\text{cc}$  but almost  $10^{21}/\text{cc}$  in AlGaAs layers.

This data was interpreted as a change in rate of chemical reactions with increasing temperature. The source for C, N, and Si in the film is the erbium precursor  $\text{Er}\{\text{N}[\text{Si}(\text{CH}_3)_3]_2\}_3$ . Residual leaks or source contaminants were the source for the oxygen. The AlGaAs layer was deposited at higher temperatures ( $720^\circ\text{C}$ ) than the GaAs layer ( $650^\circ\text{C}$ ). The erbium precursor decomposed faster at higher temperatures leaving behind copious amounts of silicon, nitrogen, and carbon. Doping of AlGaAs must be performed at lower temperatures when using erbium amides. The data implied that the level of contaminants of C, N, and Si seen in the GaAs could also be reduced at lower growth temperatures. Note that the growth temperatures used in this experiment were standard for deposition of laser structures at Spire.

When analysis of these two runs showed that erbium was incorporated into the III-V semiconductor crystal at high concentrations, proportional to the carrier flow through the erbium source, another set of deposition experiments was conducted with this erbium source to fabricate the deliverables for the first year of the program.

The deliverables were from run 2051 and 2052. Deposition steps for 2051 were identical to those in Table 3 above, lines 1, 2, 3, 5, 10 and 11. There was no buffer layer deposited, only one erbium layer (with constant carrier flow) and no capping layer. Heating and cooling cycles were as shown. For run 2052, the carrier flow of erbium was reduced to 50 sccm from the 100 sccm given in Table 3, step 5.

a.)



b.)

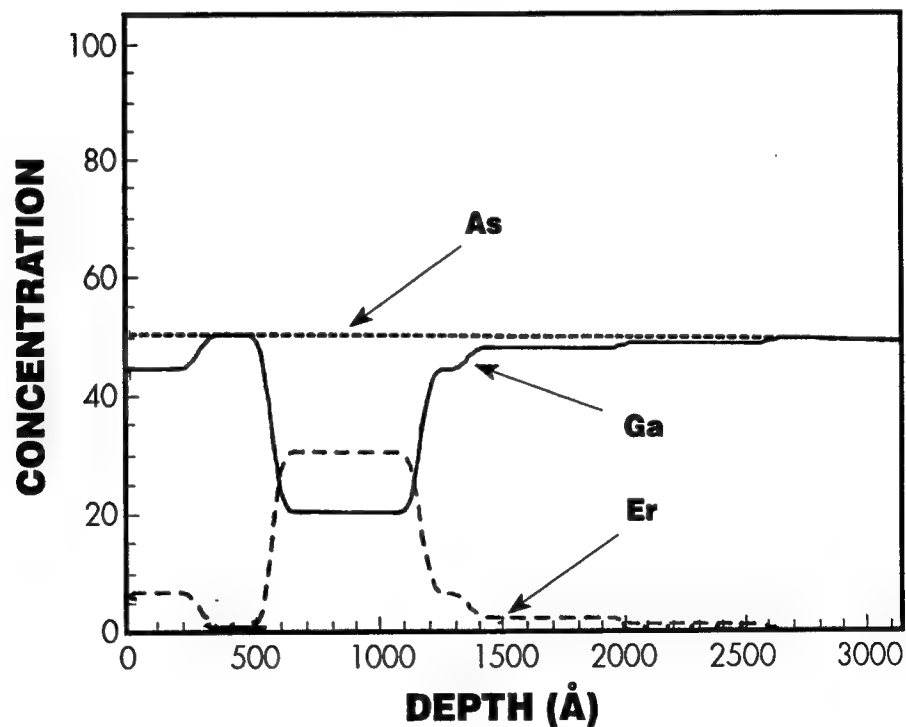


**Figure 12** RBS data (top) for sample 1941 and depth-concentration plot interpreted from data (bottom).

The surface from run 2051 was very smooth, but a slight haze was seen for run 2052. Because of the haze, run 2053 was a repeat of run 2052 and also showed a slight haze. Run 2054 repeated the work a third time but at a lower growth temperature, only 600°C instead of 650. The haze factor was greater. Analyses showed that the haze was caused by excess erbium at the start of the growth cycle. During purging of the reactor, a pressure burst from a dead space in the feed lines caused a thin layer of nearly pure erbium source material to coat the substrate at low temperatures. This layer was converted to erbium arsenide during heating, and diffused into the substrate. Lattice mismatch with the semiconductor compound layer resulted in the haze on the wafer surface. The first run, with no erbium source material in the lines at the start of the purge cycle, had a smooth surface.

Photoluminescence spectra from samples 2051 through 2054 are shown in Figure 13. As surface quality degraded with increasing number of runs (due to the initial, inadvertent doping layer) the signal strength decreased. Only samples from the first two runs were delivered to AFOSR. All samples were two-inch diameter wafers. A separate small piece, typically a quarter wafer slice, was also included for each run so that Spire would have some separate material for our own characterization, as reported below, and could deliver the entire two-inch wafer to the government.

Data for sample 2051 was verified separately by cathodoluminescence, shown in Figure 14. Additional detail at wavelengths just above 1.539 nm was observed, but not explained at this time.

Data for erbium profiles and contamination were taken again by SIMS (Figure 15) using an oxygen ion beam. For sample 2051, grown first, before saturation of the erbium carrier line, there is no deep peak at the start of growth. The erbium concentration ramps upwards with deposition time as the carrier line became saturated with the source compound, increasing the concentration of erbium in the vapor phase at the delivery point to the reactor. For sample 2052, there is a peak at the start of deposition, again due to the purging cycle. Because the erbium line was exposed to the atmosphere between each run, the carrier line had to be saturated with the source for each run. The operator typically allowed 15 minutes for this saturation to run to completion, based upon results with III-V metalorganic compounds. The slowly increasing level of erbium in the film implies that the time required for saturation with erbium amides is greater. Note especially the low levels of carbon in the film, equal to background through the film and substrate, and the lower levels of silicon, calibrated to the substrate composition.

Sample film number 2051 was also analyzed by RBS (Figure 16) and by SIMS using a cesium ion beam (Figure 17). The erbium concentration, about  $8 \times 10^{18}/\text{cc}$  agreed closely with earlier results and previous calibrations. Because this sample has a good smooth surface, the crystal structure was good and channeling analysis to determine the ratio of erbium that was substitutional in the host lattice was possible. The data indicated that about two-thirds of erbium present was on lattice sites and only one-third was interstitial. Comparison of the contamination levels to those found in sample 1941 (Figure 10), showed that the silicon and nitrogen concentrations were about a factor of ten lower while the oxygen and carbon concentrations were about the same. Deposition temperatures for sample 1941 and 2051 were identical at 650°C.

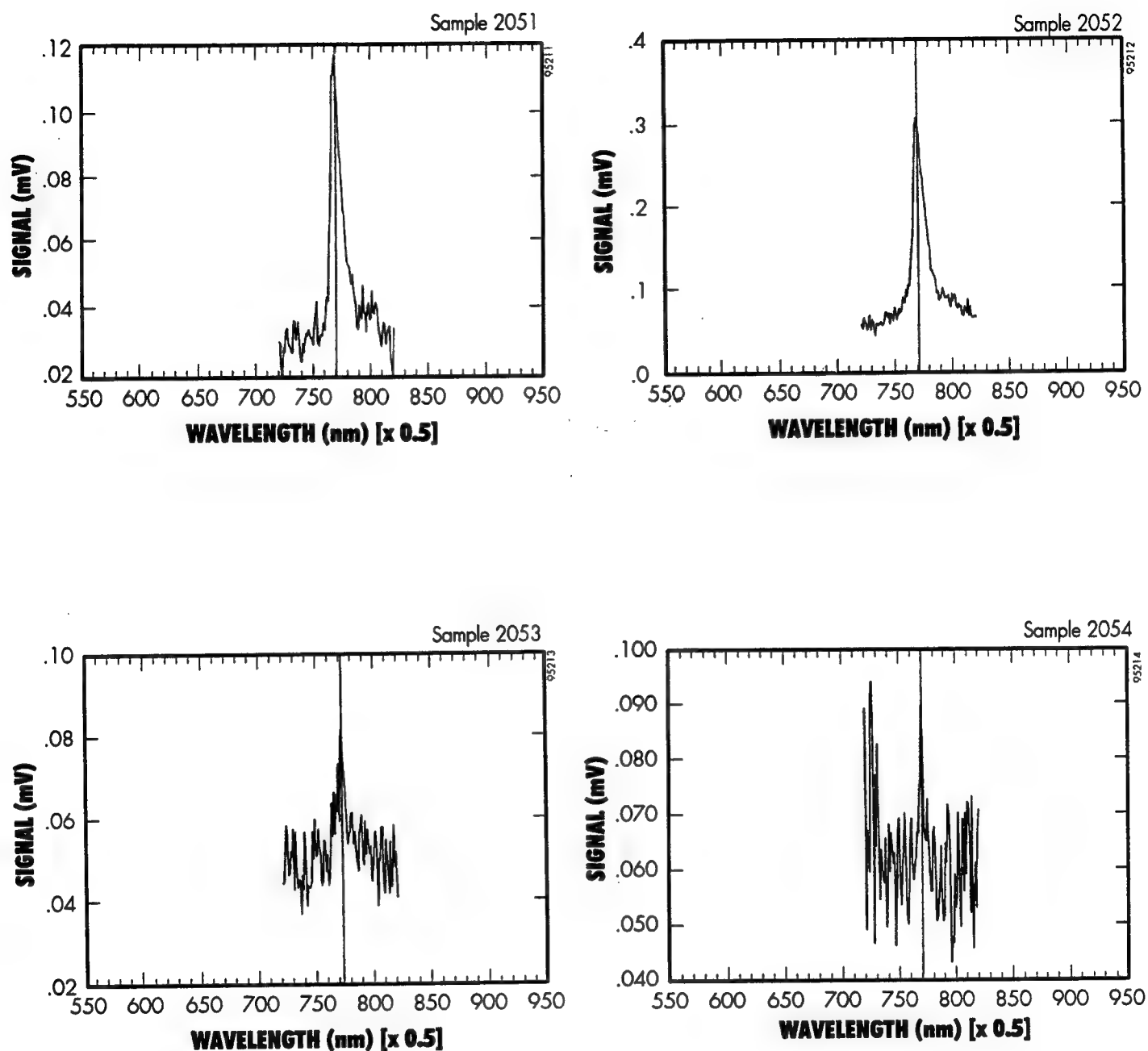


**Figure 13** *Photoluminescence data from samples 2051, 2052, 2053 and 2054 measured at 77K showing clear, sharp peak at about 1538 nm. Note that the signal strength was reduced as the level of surface haze increased.*

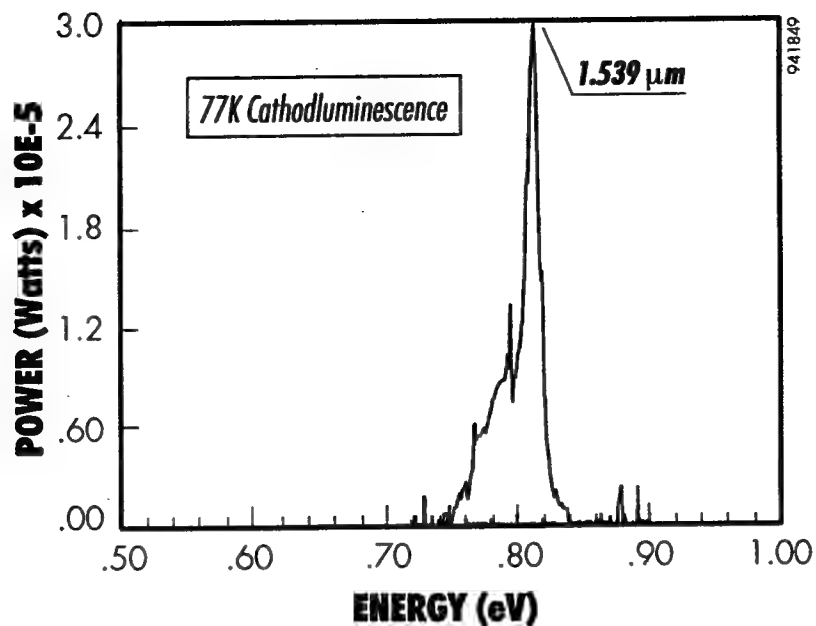


Figure 14 Cathodoluminescence spectra for sample 2051 at 77K.

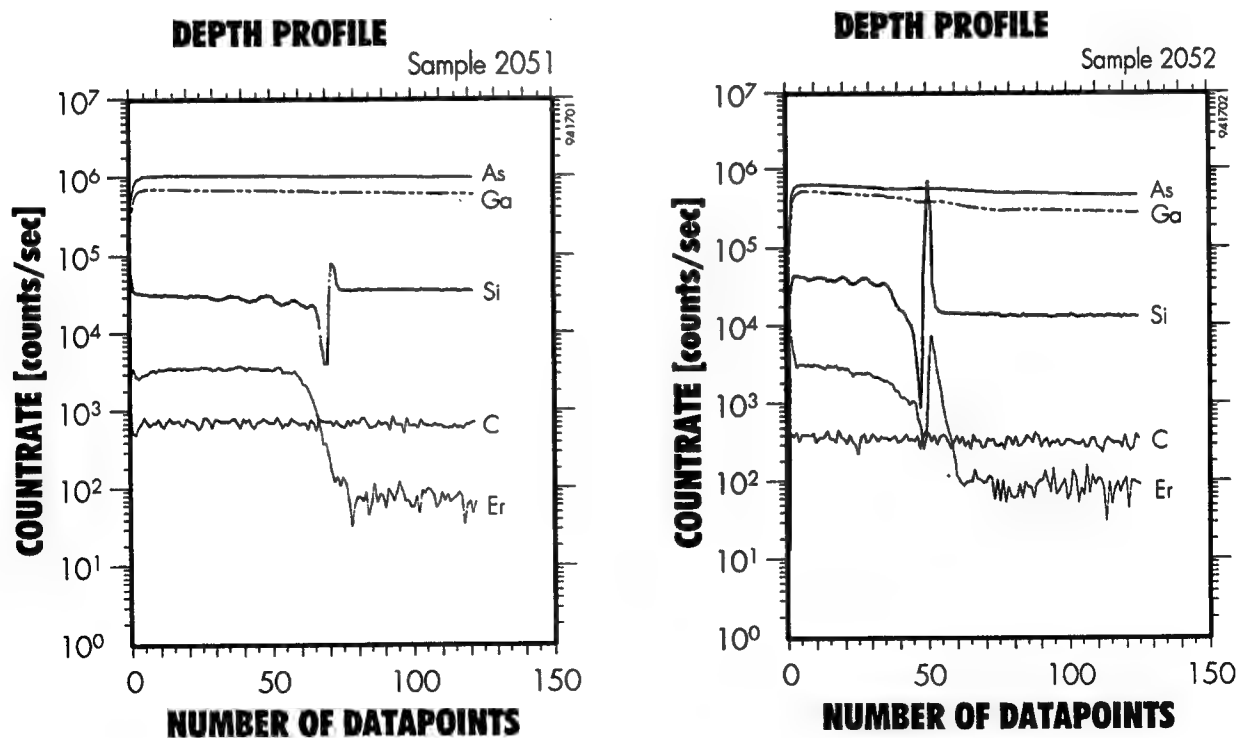


Figure 15 SIMS data using an oxygen ion beam for samples 2051 and 2052, delivered to AFOSR. Nominal erbium concentration from calibration in Figure 4c is between 6 and  $7 \times 10^{18}/\text{cc}$ .

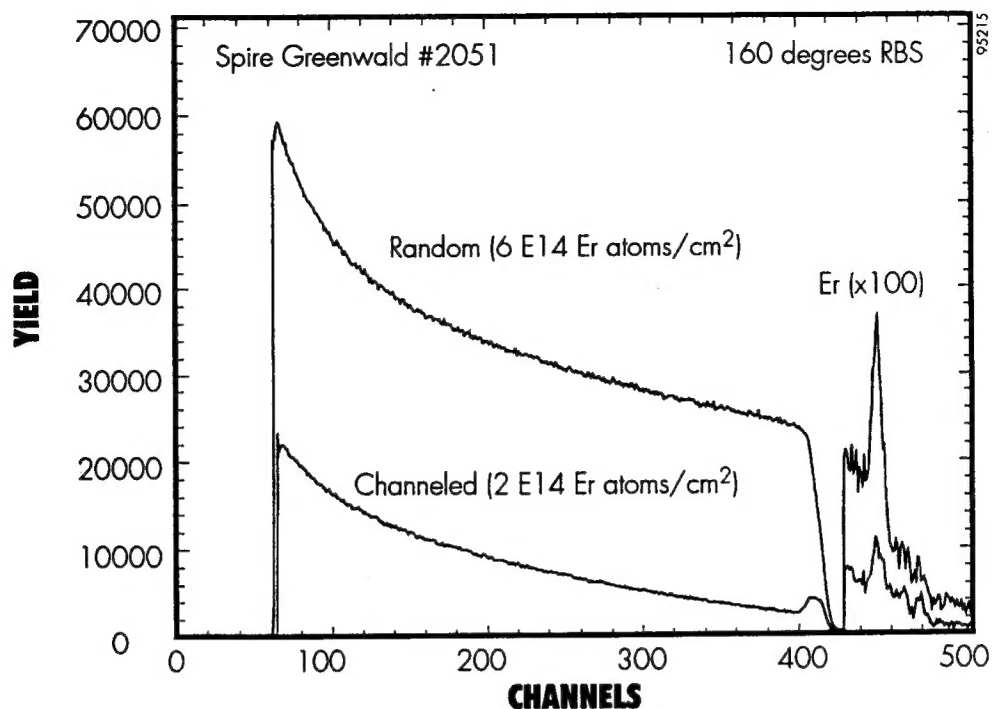


Figure 16 RBS data for sample 2051 showing random and channeling spectra, indicating % of the erbium dopant was substitutional.

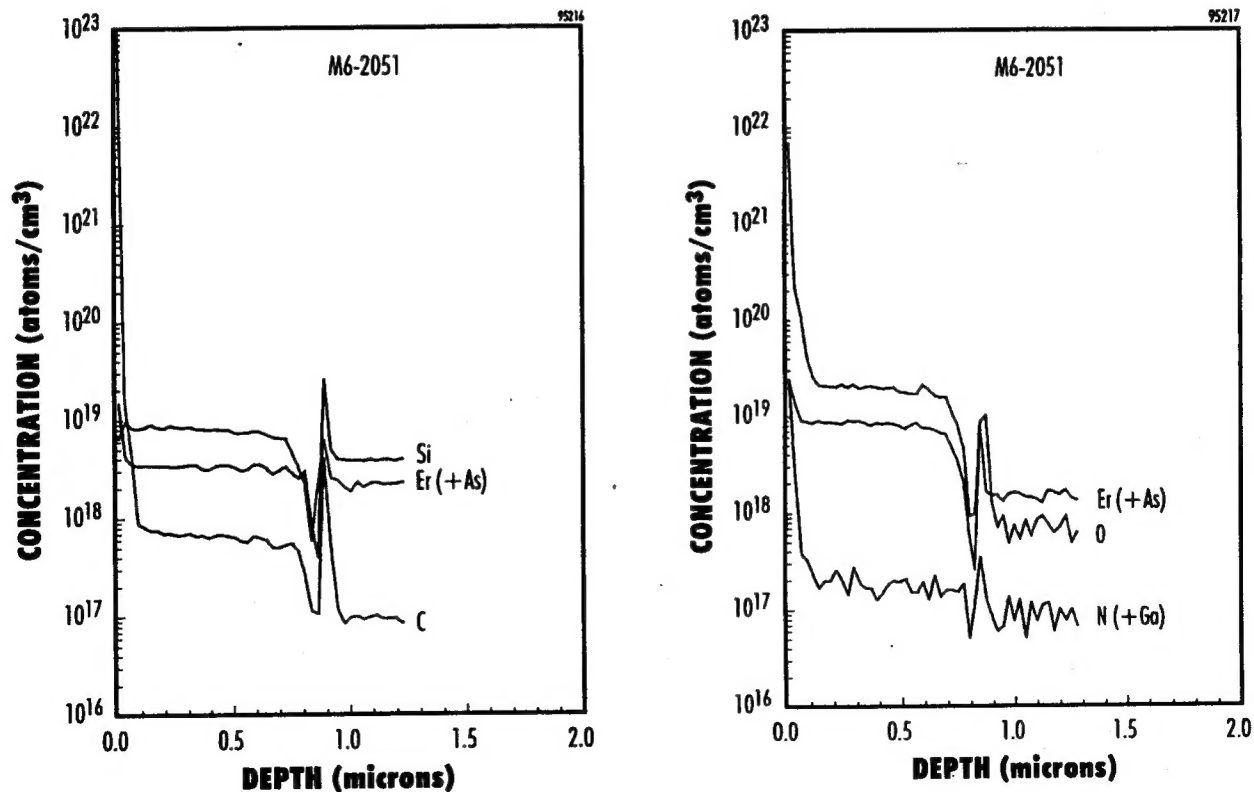


Figure 17 SIMS data of sample 2051, taken with a cesium ion beam showing oxygen and nitrogen levels (left) and silicon and carbon levels (right).

### 2.3.3 Tris-triethyldisilylamido-erbium

The objective of this set of tests was to determine if use of an alternate erbium source would reduce the amount of silicon remaining in the GaAs deposited layer when doped with erbium using disilylamines. Incorporation of silicon as a dopant in these films from the erbium source is a thermal driven chemical reaction and altering the starting point can control the results.

Nominally, it requires more energy to separate the ethyl bond from the silicon atom than the methyl bond, so that the organic radical  $\text{N} - \text{Si} - \text{Et}_2$  (where  $\text{Et}$  is  $\text{CH}_2\text{CH}_3$ ) would be expected to have slightly greater stability than the methyl substituted source radical. As the erbium source decomposes when adsorbed on the substrate surface, this greater stability of the silicon atom bonds promote formation of  $\text{NHSi}(\text{Et})_2$ . The radical continuing Si combines with the free hydrogen atoms released from arsine decomposition, instead of breaking into  $\text{C}_2\text{H}_6$  and ammonia. This should reduce the amount of silicon in the deposited film at constant temperature relative to the methyl source.

Thermal gravimetric analysis of this source was not available at the time the set of experiments was to be performed. Without reliably knowing the decomposition temperature, or the vaporization curve, the experiments tested the operating temperature of the source as the key variable. All other parameters were kept as in run 2051, the deliverable. Source temperature were slowly increased from 110 to 160°C in 10 degree steps. Photoluminescence measurements were used as a prime indicator of erbium doping. No signals were seen and the experiments were discontinued.



### SECTION 3 CONCLUSIONS

Spire successfully doped gallium-arsenide and aluminum-gallium-arsenide with erbium using disilyl-amide erbium metalorganic compounds during MOCVD growth of epitaxial layers. The erbium concentration could be varied up to 30 atomic percent, but the surface of the film remains smooth only up to a doping level of about  $10^{19}/\text{cc}$ . The erbium concentration in the delivered samples was  $8 \times 10^{18}/\text{cc}$ . Of this total, about two-thirds or over  $5 \times 10^{18}/\text{cc}$  was substitutional in the GaAs lattice.

Contamination levels were reduced in the delivered samples compared to carbon doping seen with the use of cyclopentadienyl derivatives. Typical carbon concentrations were below  $10^{18}/\text{cc}$ . Typical nitrogen concentrations were below the minimum detectable level for this technique for growth at  $650^\circ\text{C}$ . Typical silicon concentrations were below  $5 \times 10^{18}/\text{cc}$  and less than that in the substrate. Silicon incorporation varied with growth temperature, a rough plot of this variation is shown in Figure 18 below. The diffusion rate of erbium was greater than that of carbon or silicon in GaAs as determined from broadening of the curves. Estimates for diffusivity at  $650^\circ\text{C}$  were  $1 \times 10^{-15} \text{ cm}^2/\text{sec}$ .

Photoluminescence (excited by a 488 nm argon ion laser) and cathode-luminesces spectra of erbium-doped GaAs at 77K showed sharp peaks at the 1539 nm wavelength.

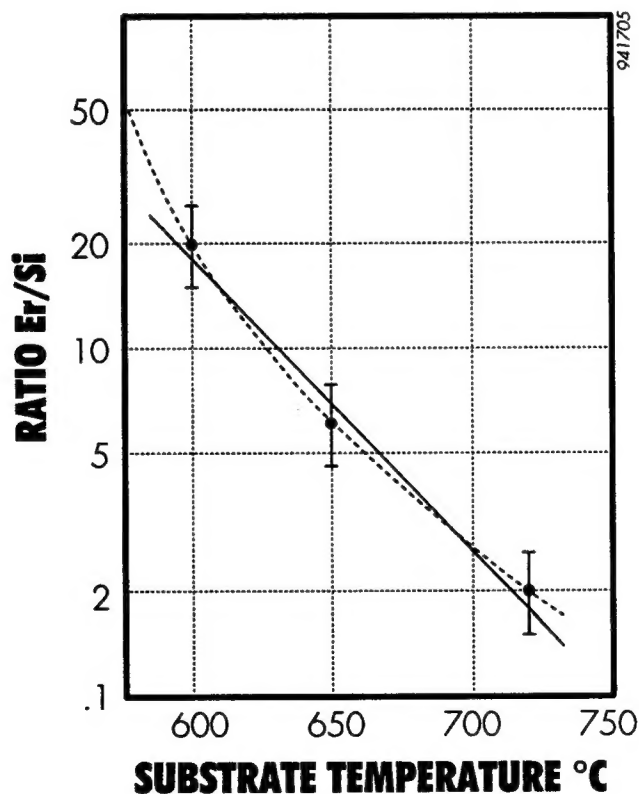


**Figure 18** Silicon doping levels as a function of growth temperature for trimethyl-disilylamido-erbium.

#### SECTION 4 REFERENCES

1. M. Kushibe *et. al.*, U.S. Patent 4,928,285 (1990), assignee Toshiba.
2. S.J. Chang and K. Takahei, *Appl. Phys. Lett.* **65**, 433 (1994).
3. H. Ennen *et. al.*, *J. Appl. Phys.*, **61**, 4877 (1987).
4. T. Bennyattou *et. al.*, *Appl. Phys. Lett.*, **60**, 350 (1992).
5. D.W. Elsaesser *et.al.*, *J. Crystal Growth*, **127**, 707 (1993).
6. Kunihiro Uwai *et. al.*, *Appl. Phys. Lett.* **51**, 1010 (1987); also, by same authors: *J. Crystal Growth*, **93**, 583 (1988).
7. Xiao M. Fang, *et. al.*, *Mat. Res. Soc. Symp. Proc.*, **301**, 15 (1993); also by same authors: *J. Appl. Phys.* **74**, 6990 (1993); also by same authors: *J. Electronic Mat.*, **23**, 1269 (1994).
8. K. Takahei, *et. al.*, *J. Appl. Phys.*, **76**, 4332 (1994).
9. D.C. Gordon, B.A. Vaartstra, T.F. Keuch and J.M. Refdwing, "Novel Organoerbium Source Reagents for MOCVD of Erbium Continuing Alloys," Final Report for contract NAS3-26708, NASA-Lewis research Center, (1993).
10. W.S. Rees, Jr, U.W. Lay and A.C. Greenwald, *Mat. Res. Soc. Symp. Proc.* , **334**, 207 (1994).